

This manuscript was accepted and published by *Industrial and Engineering Chemistry*, a journal of the American Chemical Society.

Publication data of the final, corrected work:

Becidan, M.; Várhegyi, G.; Hustad, J. E.; Skreiberg, Ø.: Thermal decomposition of biomass wastes. A kinetic study. *Ind. Eng. Chem. Res.* **2007**, 46, 2428-2437. doi: [10.1021/ie061468z](https://doi.org/10.1021/ie061468z)

---

# Thermal Decomposition of Biomass Wastes. A Kinetic Study

*Michaël Becidan<sup>†</sup>, Gábor Várhegyi<sup>‡\*</sup>, Johan E. Hustad<sup>†</sup>, Øyvind Skreiberg<sup>†</sup>*

<sup>†</sup> NTNU, Department of Energy and Process Engineering,  
Kolbjørn Hejes vei 1A, NO-7491 Trondheim, Norway.

<sup>‡</sup> Institute of Materials and Environmental Chemistry, Chemical Research Center,  
Hungarian Academy of Sciences, P.O. Box 17, Budapest 1525, Hungary.

\* To whom correspondence should be addressed.

Email: [varhegyi.gabor@t-online.hu](mailto:varhegyi.gabor@t-online.hu) or [gvarhegyi@gmail.com](mailto:gvarhegyi@gmail.com)

**ABSTRACT.** Wastes from brewery, industrial coffee roasting and fiberboard furniture were investigated. Thermogravimetric experiments were carried out with different types of temperature programs. Three models were proposed describing equally well the behavior of the samples. One of the models consisted of three partial reactions with distributed activation energies (DAEM). In this case 12 parameters were sufficient to describe the behavior of a sample in the whole range of observations. The other two models were mathematically simpler, but contained higher numbers of adjustable parameters. The reliability of the models was tested in three ways: (i) the models provided good fit for all experiments; (ii) the evaluation of a narrower subset of the experiments resulted in approximately the same parameters as the evaluation of the whole series of experiments; (iii) the models allowed accurate extrapolations to higher heating rates.

**Keywords:** Brewery spent grains (BSG); coffee waste; middle density fiberboard (MDF); thermogravimetry (TGA); distributed activation energy (DAEM); model validation; constant reaction rate experiments (CRR).

## 1. Introduction

The replacement of fossil fuels by alternative energy sources has an increasing importance nowadays. The use of various plant materials (biomass) for energy production has a major contribution to this task since biomass is renewable and its increased utilization reduces the CO<sub>2</sub> emission of the energy sector. There is a wide range of biomass-type wastes that are not yet properly utilized. The study of their properties from the points of view of combustion, gasification, pyrolysis and other thermochemical utilization processes is an important research direction.<sup>1-7</sup> Thermogravimetric analysis (TGA) has proved to be a useful tool in such studies. It provides information on the partial processes and reaction kinetics. TGA was frequently employed in the kinetic modeling of the thermal degradation of biomass-type wastes.<sup>8-22</sup>

There is a vast literature on the kinetic evaluation methods of thermal analysis from its beginnings in the fifties to the present. A general survey is outside the scope of the present work. We list here a few recent general reviews, and add more citations in the discussion. A detailed review was published by Burnham and Braun on the kinetic analysis of complex materials, where the term “complex” referred to the complexity of the physical and chemical structure of the samples.<sup>23</sup> Caballero and Conesa published mathematical considerations for non-isothermal kinetics that involves, among others, the simultaneous evaluation of series of experiments using complex models and the method of least squares.<sup>24</sup> The kinetic evaluation methods used in our work were recently surveyed by Várhegyi.<sup>25</sup>

In the present work we report results on the devolatilization kinetics of three biomass wastes: brewer spent grains (BSG), coffee waste and fiberboard. These wastes are produced all over the world in large quantities while their optimal utilization has not been found yet. BSG is the main brewery by-product with 0.03 kg dry BSG produced per liter beer.<sup>26</sup> As the yearly worldwide beer production is about 160 billion liters,<sup>27</sup> roughly 5 million metric tons of dry BSG forms yearly. The coffee waste used in this study is collected during green coffee roasting and was evaluated to represent 1.5 wt% of pre-roasted green coffee. The coffee industry produces ca. 0.1 million tons of this waste yearly. Fiberboard, consisting mainly of wood, is produced in huge quantities. The worldwide production of medium density fiberboard (MDF) is about 40 million m<sup>3</sup>.<sup>28</sup> Besides the fiberboard wastes of the furniture industry, all fiberboard furniture will eventually be turned into wastes that may be considered in the optimal waste utilization strategies. Few data have been published on the potential utilization and thermal properties of these wastes.<sup>2,26,29-34</sup> We did not find publications discussing their devolatilization kinetics.

From a chemical point of view, the studied samples cover a wide range of biomass wastes. Brewery spent grains are composed mainly from proteins, hemicellulose, lignin and starch with smaller amounts of cellulose and lipids.<sup>26,29,35</sup> Coffee wastes contain mainly sugars, lipids and proteins with smaller amounts of alkaloids and other plant materials.<sup>36</sup> Fiberboard is made from wood fiber (recycled and recovered wood waste) and a resin to bind the wood fibers together. Usually urea-formaldehyde resin is used; its concentration in MDF is around 8-10%.<sup>33</sup>

The present work aims at obtaining dependable information on the behavior of selected biomass wastes during heating. Models, evaluation methods and validation strategies are outlined to describe their

devolatilization in a wide domain of temperature – time functions. Since the treatment proved to be valid for biomass wastes of very different chemical compositions, the considerations of the paper may be recommended to other investigators of the field, too. The study was strictly restricted to the regime of the kinetic control: the sample size, particle sizes and heating programs were chosen so that the various transport processes would be negligible. Accordingly, the results cannot be directly employed in industrial process and reactor design; instead of this they aim only at providing guidance for the further work in this area.

## 2. Experimental

**2.1. Samples.** A middle density fiberboard sample (MDF) was obtained from IKEA AS, Norway. This material is produced from wood wastes (pine and spruce) and ca. 10% urea - formaldehyde resin. Its specific density was 703 kg/m<sup>3</sup>. Brewer spent grains (BSG) were provided by Carlsberg Brewery, Denmark. Coffee wastes (CW) were received from Kjeldsberg Kaffebrønnen AS, Norway. This substance consists of skin, silverskin, pulp, parchment, and broken beans that are lost during the roasting process.

The proximate and ultimate analyses of the samples can be found in Table 1. The samples exhibit the usual properties of biomass materials. Their nitrogen content is remarkably high, which is due to proteins in the case of BSG, proteins and alkaloids in CW, while the nitrogen content of MDF arises almost entirely from the urea-formaldehyde resin.

The samples were ground and sieved. The fraction of 45 - 63  $\mu\text{m}$  was used for the TGA experiments. The use of small particle sizes ensures the kinetic control by eliminating diffusion and heat transfer problems inside the particles. The omission of the finest particles eliminated the problems of dusts blown out by the gas stream during the experiments.

**Table 1. Main physical and chemical properties of the samples**

	BSG	CW	MDF
Proximate analysis (wt%, dry basis)			
Volatile matter	78.75	76.67	81.95
Fixed carbon	16.22	16.75	17.61
Ash	5.03	6.58	0.44
Ultimate analysis (wt%, dry ash free basis)			
Carbon	51.59	51.33	48.80
Hydrogen	7.07	6.79	6.33
Nitrogen	4.15	3.02	3.62
Sulfur	0.23	0.21	<0.02
Oxygen (by difference)	36.96	38.65	41.25

**2.2. Thermogravimetric experiments.** A TA Instruments Q500 TGA thermal analysis system was employed. Low sample masses were used to reduce the heat transfer problems of thermal analysis. Approximately 5 mg biomass was evenly distributed in a Pt sample pan of  $\varnothing$  9.6 mm. Smaller sample mass, about 2.5 mg, was used at the highest heating rate of this study (20°C/min). The measurements were carried out in 100 ml/min high purity nitrogen gas flow. Each experiment was started with a 30 min purging period at room temperature and a 30 min drying period at 105°C and was terminated around 600°C (final temperature hold for 20 min). The kinetic evaluation started after the drying, when the sample reached 120°C. This point was set as  $t=0$  in the figures of the paper.

Five experiments were carried out with each biomass at different heating programs in order to provide a sufficient amount of information for the kinetic modeling. The temperature – time functions are shown in Figure 1. One experiment for each sample utilized the “constant reaction rate” (CRR) capabilities of the equipment. When the reaction rate achieved a preset level in these experiments, the furnace temperature was regulated in such a way that the reaction rate fluctuated around a constant level. The CRR experiments resulted in evenly low reaction rates in the whole domain. As it will be shown later in the paper, the corresponding DTG curves (experimental  $-dm/dt$  vs. time functions) strongly differed from the other experiments and, in this way, highly increased the information content of the series evaluated.

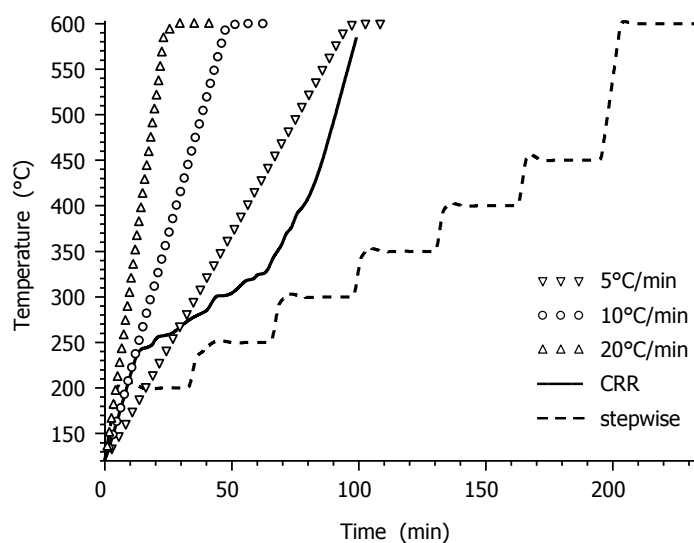


**Figure 1.** Temperature – time functions used in the study. The  $T(t)$  function of the “constant reaction rate” (CRR) experiment belongs here to BSG.

A stepwise experiment was carried out for each sample. It consisted of 30 min isothermal sections at 200, 250, 300, 350, 400, 450 and 600°C, as shown in Figure 1. (It also included the drying section at 105°C.) The isothermal sections were connected by 20°C/min heating ramps. The aim of the stepwise experiments was to include isothermal sections and relatively fast temperature rises into the kinetic evaluation. Experiments with linear heating programs were also carried out at heating rates of 5, 10 and 20°C/min.

**Table 2. Characteristics of the thermogravimetric experiments**

Sample	T(t)	time span <sup>a</sup> (min)	mean -dm/dt <sup>a</sup> (s <sup>-1</sup> ) ×1000	max -dm/dt (s <sup>-1</sup> ) ×1000	T <sub>peak</sub> (°C)	Residue (%)
BSG	5°C/min	33	0.32	0.51	281	22
BSG	10°C/min	17	0.63	0.99	292	21
BSG	20°C/min	8	1.32	2.16	298	20
BSG	CRR <sup>b</sup>	64	0.16	0.23	(299)	22
BSG	stepwise	98	0.11	0.64	291	22
CW	5°C/min	38	0.24	0.53	315	30
CW	10°C/min	20	0.49	1.02	325	29
CW	20°C/min	10	0.99	2.05	332	29
CW	CRR <sup>b</sup>	59	0.15	0.21	(233)	31
CW	stepwise	128	0.07	0.50	293	30
MDF	5°C/min	25	0.45	0.73	344	17
MDF	10°C/min	12	0.89	1.40	354	17
MDF	20°C/min	6	1.77	2.72	367	16
MDF	CRR <sup>b</sup>	65	0.17	0.24	(264)	19
MDF	stepwise	86	0.13	0.75	344	18

<sup>a</sup> The time span was characterized by the interval between 10 and 90% of the overall mass loss. The mean of  $-dm/dt$  also refers to this domain.

<sup>b</sup> CRR: Constant reaction Rate (see text for description). The corresponding T<sub>peak</sub> temperatures were parenthesized since the CRR regulation results in reaction rates fluctuating around a preset level.

The main characteristics of the experiments are summarized in Table 2. The time span was characterized by the interval between 10 and 90% of the overall mass loss. The average reaction rates are also given in these domains. The table indicates 10 - 14 times variation in the time span, mean reaction rate and peak reaction rate for each sample, reflecting the wide range of experimental conditions employed in the study.

It is interesting to note that the residue values did not show a large variation with the heating programs. As Fig. 1 shows, all experiments were terminated by an isothermal section at 600°C except the CRR experiments which ended at a slightly lower T without an isothermal section. (This was due to technical reasons.) Nevertheless, the residues of the CRR and the similarly slow stepwise T(t) experiments were close to each other. It is well known that several organic materials give lower char yield at higher heating rates.<sup>37,38</sup> We also observed that the char yields at 20°C are lower than the values belonging to the 5°C/min, stepwise T(t) and CRR experiments. However, the differences were low. Accordingly, no term was involved into the models to describe the variation of the char yield with the type of the temperature program.

The repeatability of the thermogravimetric experiments have been treated many times in the literature. Mészáros *et al.* have reported good repeatability on sample sizes as low as 0.2 mg in the case of a biomass sample containing bark, heart-, and sapwood.<sup>39</sup> In the present work we checked the repeatability on the coffee waste sample at 10°C/min. The root means square (rms) difference between the  $-dm/dt$  data were calculated in the interval used for the kinetic evaluation. Expressed as a percent of the peak maxima, this

quantity was 0.9%. The noise of the  $-dm/dt$  curves had a significant role in this value. The rms difference between the two  $-dm/dt$  curves proved to be smaller, 0.4%, in a test calculation when the smoothing in the determination of  $-dm/dt$  was stronger than our usual procedure.<sup>40</sup>

### 3. Results and discussion

**3.1. Simultaneous evaluation by the method of least squares.** Fortran 95 and C++ programs developed by one of the authors were employed.<sup>8,20,25,41,42</sup> The models discussed in the next sections were used to simulate TG and DTG curves at all  $T(t)$  of this study. The unknown parameters were determined by the method of least squares. As presented above, we had five different experiments for each sample. The experiments on a given sample were evaluated simultaneously by comparing the normalized mass loss rates,  $(-dm/dt)^{obs}$ , to their simulated counterparts,  $(-dm/dt)^{calc}$ :

$$S = \sum_{k=1}^{N_{exp}} \sum_{i=1}^{N_k} \frac{\left[ \left( \frac{dm}{dt} \right)_k^{obs}(t_i) - \left( \frac{dm}{dt} \right)_k^{calc}(t_i) \right]^2}{N_k h_k^2} \quad (1)$$

Subscript  $k$  indicates the different experiments.  $N_{exp}$  is the number of experiments evaluated simultaneously,  $t_i$  denotes the time values in which the digitized  $(dm/dt)^{obs}$  values were taken, and  $N_k$  is the number of the  $t_i$  points in a given experiment.  $h_k$  denotes the heights of the evaluated curves that strongly depend on the experimental conditions. The division by  $h_k^2$  serves for normalization. The fit was characterized by the following quantity:

$$fit (\%) = 100 S^{0.5} \quad (2)$$

Eq. 2 is also employed to express the fit of a single experiment within the evaluated group. In such cases the first sum is omitted in eq. 1.

**3.2. Model validation.** It is well known that the most important components of the thermoanalytical experiments are not random. Accordingly, the methods of mathematical statistics cannot be employed to test the goodness of a model. We used three ways to test the reliability and usefulness of a model:

(i) the models should provide good fits for all experiments in the wide range of experimental conditions outlined in Table 2;

(ii) the evaluation of a narrower subset of the experiments (the three slowest experiments) should provide approximately the same parameters as the evaluation of the whole series of experiments;

(iii) the models should be able to predict the behavior of the samples outside of the experimental conditions at which the model parameters were determined.

The first criterion was satisfied by the simultaneous evaluation of the experiments by the method of least squares. The number of partial reactions was gradually increased in each model until a good fit was observed for all experiments.

The second and third criteria were checked so that the three slowest experiments were evaluated in test calculations. As Table 2 shows, these are the “constant reaction rate” experiments and the experiments carried out at stepwise  $T(t)$  and at  $5^\circ\text{C}/\text{min}$ . The corresponding time-spans, as defined in Table 2, varies from 25 to 128 minutes. (The results of these test calculations are shown later in the text, in Section 3.6.) In the next step of the calculations it was checked how the fastest experiment on each sample can be described by the parameters obtained from the three slowest experiments. Accordingly,  $-\text{dm}/\text{dt}$  curves were simulated for the  $T(t)$  functions of the  $20^\circ\text{C}/\text{min}$  experiments using the parameters obtained from the slow experiments and these simulated curves were compared to the observed  $-\text{dm}/\text{dt}$  data at  $20^\circ\text{C}/\text{min}$  heating rate. As Table 2 shows, this procedure is an extrapolation to ca. four-time higher reaction rates from the domain of the three slowest experiments. This reliability test is an extension of an earlier work of Várhegyi *et al.*<sup>42</sup>

**3.3. First-order model.** Independent first order reactions are frequently used for the description of biomass devolatilization.<sup>8,13,20,39,43-48</sup> As an approximation, we regard a sample to be composed from pseudocomponents, where a pseudocomponent is a group of reactive species that exhibit similar reactivity. A first order kinetic equation is assumed for each pseudocomponent that defines the time and temperature dependence of the reacted fractions  $\alpha_j$ :

$$d\alpha_j/dt = A_j e^{-E_j/RT} (1-\alpha_j) \quad (3)$$

Here  $A_j$  is the pre-exponential factor and  $E_j$  is the activation energy. We use the IUPAC terminology for the activation energy: it is an empirical parameter characterizing the exponential temperature dependence of the rate coefficient.<sup>49</sup> The resulting mass loss rate curve is the weighted sum of the individual  $d\alpha_j/dt$  reaction rates:

$$-\text{dm}/\text{dt} = \sum_{j=1}^{N_{comp}} c_j d\alpha_j / dt \quad (4)$$

where  $m$  is the normalized sample mass,  $N_{comp}$  is the number of pseudocomponents, and  $c_j$  is the normalized mass of volatiles formed from pseudocomponent  $j$ .

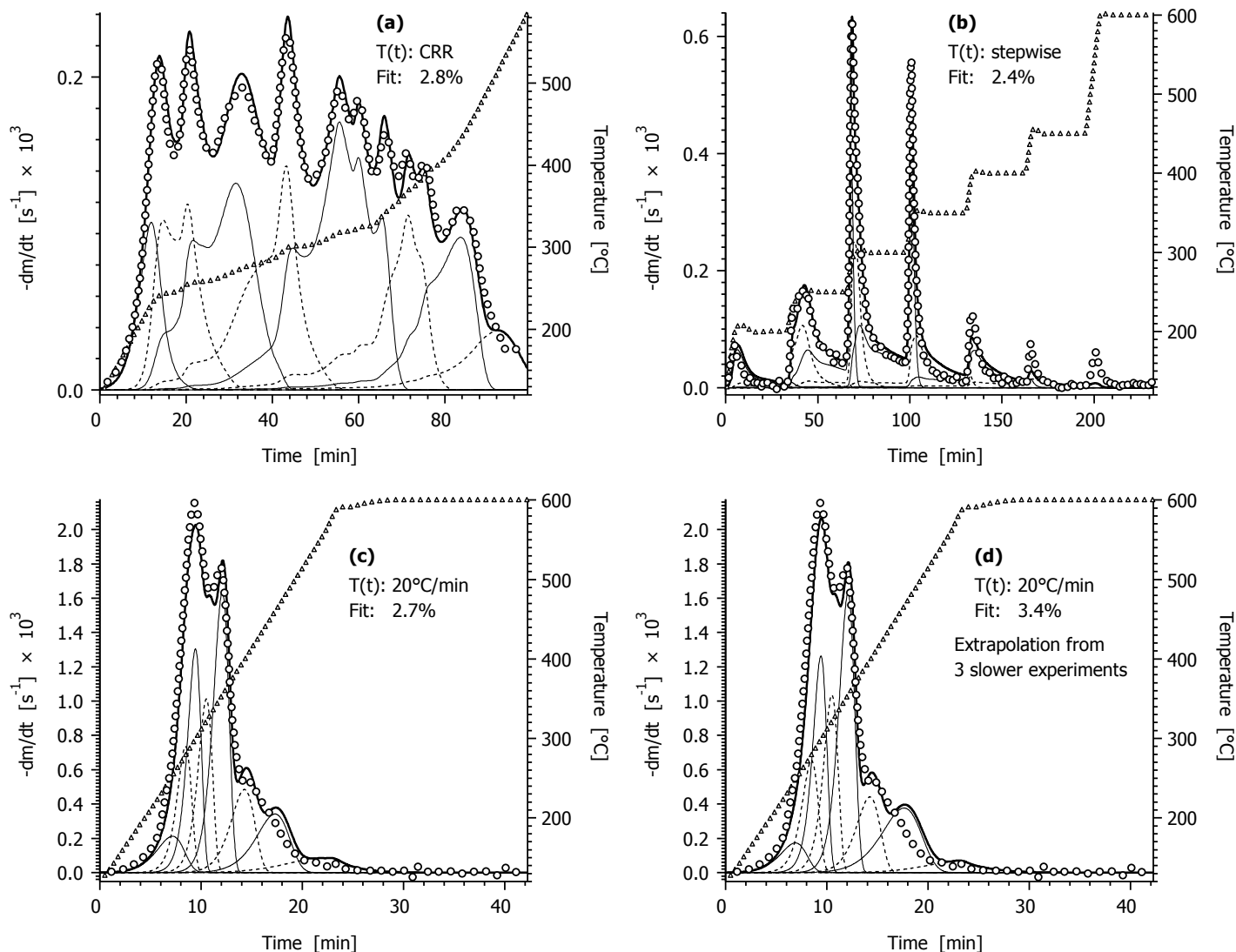


**Figure 2.** Description of the devolatilization of the BSG sample by eight first order reactions. Panels (a) – (c) show results obtained from the simultaneous evaluation of 5 experiments. Panel (d) illustrates how the fastest experiment can be described by parameters obtained from three slow experiments. Notation:  $T(t)$  function ( $\Delta$ ); experimental  $-dm/dt$  (o); simulated  $-dm/dt$  (—); partial curves (— and - - -, every 2<sup>nd</sup> partial curve is dashed for a better visibility).

As Figure 2 shows, it was possible to obtain good fits with this model, and the extrapolation test gave also good results. However, 7 – 8 partial reactions had to be assumed in this model. (Lower numbers of partial reactions did not result in acceptable fits.) The reasons for this high number may be due to the following two factors:

(i) The wastes studied in the present work are particularly inhomogeneous materials. They are composed from chemically and physically different parts of the plants. Besides, BSG arises from different plants (barley, maize, hop) and contains microorganisms and enzymes. Similarly, MDF is made from different woods and a considerable amount of urea resin, and it includes some bark, too.

(ii) We required the description of the devolatilization at an unusually wide range of  $T(t)$  programs, as seen in Figures 1 and 2.

The corresponding kinetic parameters are listed in Table 3.

**Table 3. Parameters of the 1<sup>st</sup> order model**

Sample	BSG	CW	MDF
<i>Fit</i> / %	2.4	2.7	2.1
$E_1$ / kJ mol <sup>-1</sup>	84	106	88
$E_2$ / kJ mol <sup>-1</sup>	172	173	150
$E_3$ / kJ mol <sup>-1</sup>	197	185	177
$E_4$ / kJ mol <sup>-1</sup>	200	206	190
$E_5$ / kJ mol <sup>-1</sup>	206	206	183
$E_6$ / kJ mol <sup>-1</sup>	157	138	148
$E_7$ / kJ mol <sup>-1</sup>	134	108	76
$E_8$ / kJ mol <sup>-1</sup>	85	100	—
$\log_{10} A_1/s^{-1}$	6.40	8.72	7.07
$\log_{10} A_2/s^{-1}$	14.66	14.79	12.51
$\log_{10} A_3/s^{-1}$	16.39	15.04	14.28
$\log_{10} A_4/s^{-1}$	15.92	16.04	14.78
$\log_{10} A_5/s^{-1}$	15.42	15.40	13.23
$\log_{10} A_6/s^{-1}$	10.31	8.76	9.08
$\log_{10} A_7/s^{-1}$	7.53	5.43	2.48
$\log_{10} A_8/s^{-1}$	3.08	3.79	—
$c_1$	0.04	0.06	0.04
$c_2$	0.08	0.09	0.06
$c_3$	0.14	0.10	0.09
$c_4$	0.11	0.18	0.14
$c_5$	0.20	0.08	0.38
$c_6$	0.09	0.07	0.05
$c_7$	0.09	0.08	0.05
$c_8$	0.04	0.04	—

**3.4.  $n$ th order model.** In the previous section we employed first order kinetics for the partial reactions. The first order approximation assumes that each reacting species of a given pseudocomponent reacts with the same probability. However, the biomass wastes are strongly inhomogeneous materials where the reactivity of a given chemical structural unit may depend on its physical position and chemical environment. The application of power-law functions ( $n$ th order kinetics) is a simple way to approximate formally the differences between the fractions of a given pseudocomponent:

$$d\alpha_j/dt = A_j e^{-E_j/RT} (1-\alpha_j)^{n_j} \quad (5)$$

where  $n_j$  is the order of reaction. This approximation is frequently employed for the description of biomass materials.<sup>18,19,39,45,50</sup> According to the IUPAC definition, the orders of reaction “can be positive or negative integral or rational nonintegral numbers”.<sup>49</sup> Nevertheless, we employed the following restriction

$$0 \leq n_j \leq 3 \quad (6)$$

since  $n_j$  values outside of this interval results in  $-dm/dt$  curves with unrealistic shapes.

Using the  $n$ th order kinetics (equations 4, 5 and 6), the assumption of four partial reactions was sufficient for a good fit, as illustrated in Figure 3.

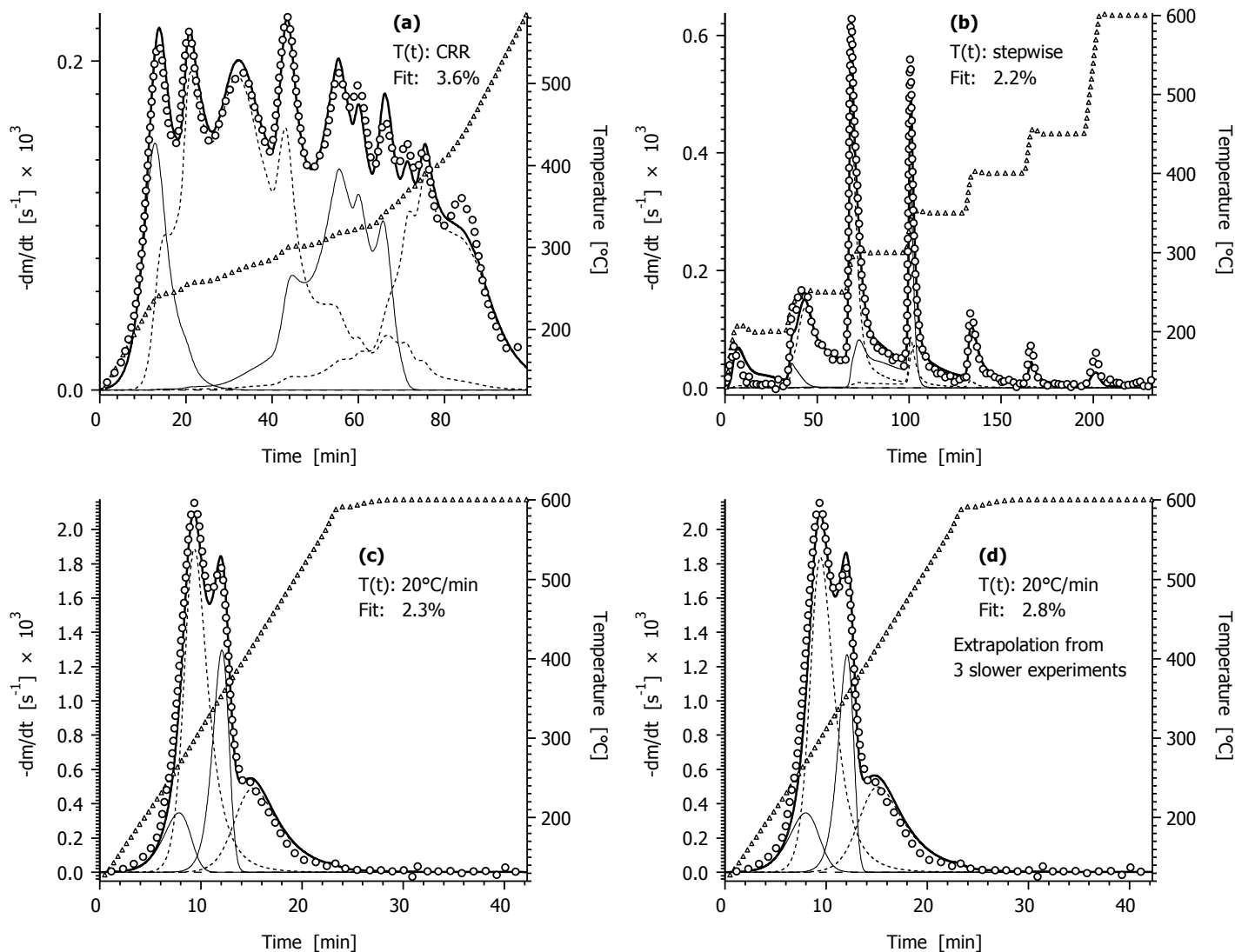


**Figure 3.** Description of the devolatilization of the BSG sample by four  $n$ th order reactions. (See Figure 2 for notes and line-styles.)

The extrapolation test gave favorable results with this model, too, as illustrated in panel (d) of Figure 3. The corresponding parameters are listed in Table 4.

**Table 4. Parameters of the  $n$ th order model**

Sample	BSG	CW	MDF
<i>Fit</i> / %	2.4	2.4	2.6
$E_1$ / kJ mol <sup>-1</sup>	91	118	81
$E_2$ / kJ mol <sup>-1</sup>	199	203	178
$E_3$ / kJ mol <sup>-1</sup>	212	214	180
$E_4$ / kJ mol <sup>-1</sup>	156	125	106
log <sub>10</sub> $A_1$ /s <sup>-1</sup>	6.91	10.17	5.64
log <sub>10</sub> $A_2$ /s <sup>-1</sup>	16.58	17.61	13.82
log <sub>10</sub> $A_3$ /s <sup>-1</sup>	15.94	16.79	12.85
log <sub>10</sub> $A_4$ /s <sup>-1</sup>	9.88	7.10	5.30
$n_1$	1.09	1.34	1.29
$n_2$	3.00	3.00	3.00
$n_3$	1.13	1.98	0.80
$n_4$	3.00	3.00	3.00
$c_1$	0.07	0.06	0.12
$c_2$	0.37	0.20	0.36
$c_3$	0.16	0.28	0.27
$c_4$	0.18	0.16	0.07

**3.5. Distributed activation energy model.** The chemical and physical differences of the reactive species can frequently be described by distributed activation energy models (DAEM), as Burnham and Braun outlined in a detailed review in 1999.<sup>23</sup> In the simplest sort of DAEM the distribution of the activation energy is approximated by a Gaussian distribution, and the reaction rate depends on the amount of reactant by 1<sup>st</sup> order kinetics. Later Várhegyi *et al* employed this type of model to describe samples by more than one partial reaction.<sup>42</sup> This approach shall be followed in the present work. Assuming that the reacting species differ from each other within a given pseudocomponent, we shall approximate non-uniformity by a  $D_j(E)$  distribution of the activation energy. Let  $\alpha_j(t,E)$  denote the solution of a first order kinetic equation at a given  $E$  value:

$$d\alpha_j(t,E)/dt = A_j e^{-E/RT} [1-\alpha_j(t,E)] \quad (7)$$

The distribution of  $E$  is described by a Gaussian distribution function:

$$D_j(E) = (2\pi)^{-1/2} \sigma_j^{-1} \exp[-(E-E_{0,j})^2/2\sigma_j^2] \quad (8)$$

where  $E_{0,j}$  and  $\sigma$  are the mean value and the width-parameter (variation) of the distribution. The overall reacted fraction of the  $j$ th pseudocomponent is obtained by integration:

$$\alpha_j(t) = \int_0^{\infty} D_j(E) \alpha_j(t,E) dE \quad (9)$$

The details of the evaluation by this type of model can be found in the work of Várhegyi *et al*.<sup>42</sup> Using the DAEM model, the assumption of three partial reactions were sufficient for a good fit in the entire domain of

observations, and the extrapolation tests gave also satisfying results, as shown in Figures 4 – 6. The corresponding parameters are listed in Table 5.

**Table 5. Parameters of the distributed activation energy model**

Sample	BSG	CW	MDF
<i>Fit</i> / %	1.9	2.0	2.9
$E_{0,1}$ / kJ mol <sup>-1</sup>	218	236	209
$E_{0,2}$ / kJ mol <sup>-1</sup>	221	222	180
$E_{0,3}$ / kJ mol <sup>-1</sup>	213	224	175
$\log_{10} A_1/s^{-1}$	18.34	20.90	16.84
$\log_{10} A_2/s^{-1}$	16.80	17.39	12.93
$\log_{10} A_3/s^{-1}$	15.73	16.07	12.64
$\sigma_1$	7.8	11.8	12.4
$\sigma_2$	0.0	4.5	0.0
$\sigma_3$	27.2	32.4	33.3
$c_1$	0.25	0.20	0.32
$c_2$	0.13	0.23	0.30
$c_3$	0.40	0.27	0.20

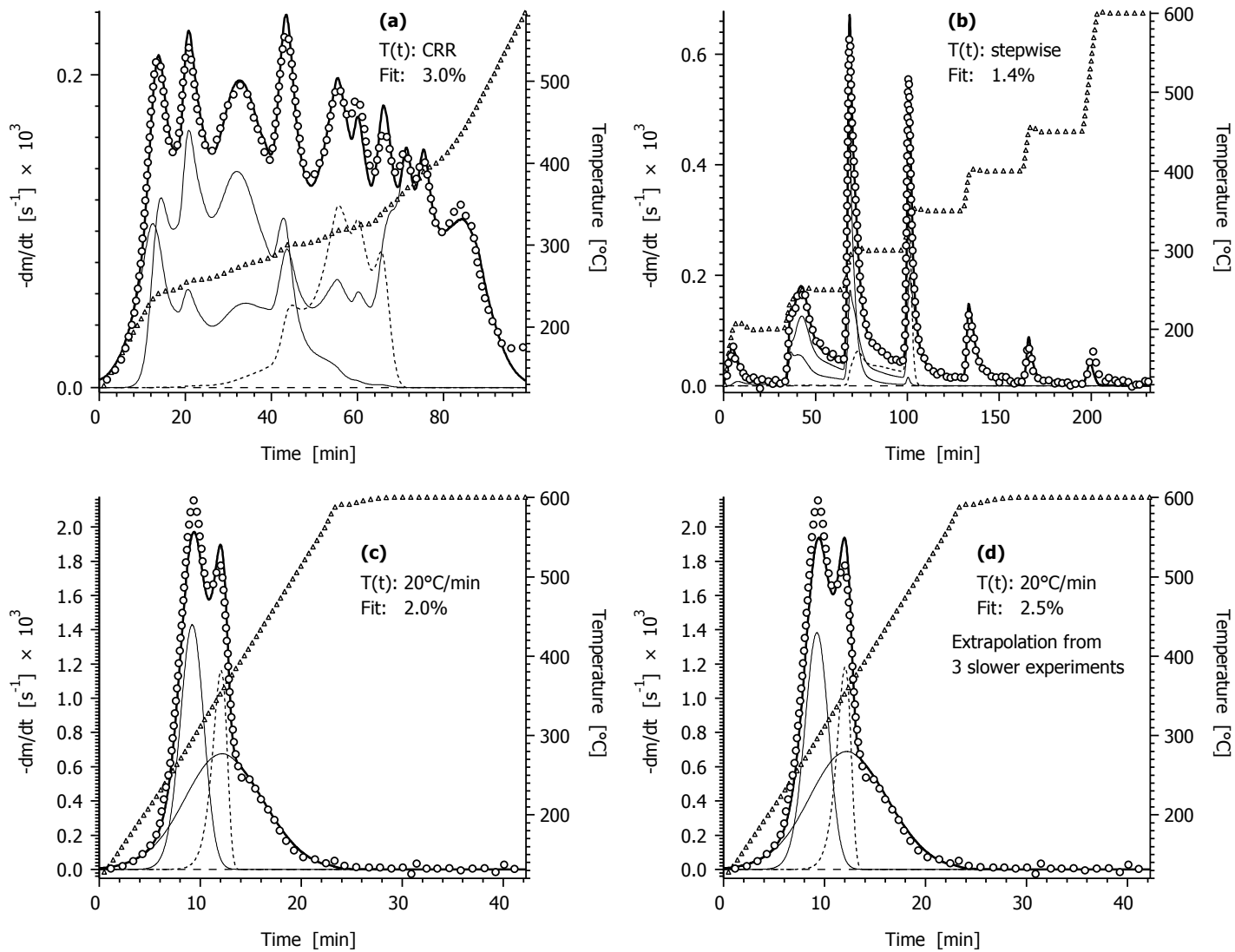


**Figure 4.** Description of the devolatilization of the BSG sample by three DAEM reactions. (See Figure 2 for notes and line-styles).

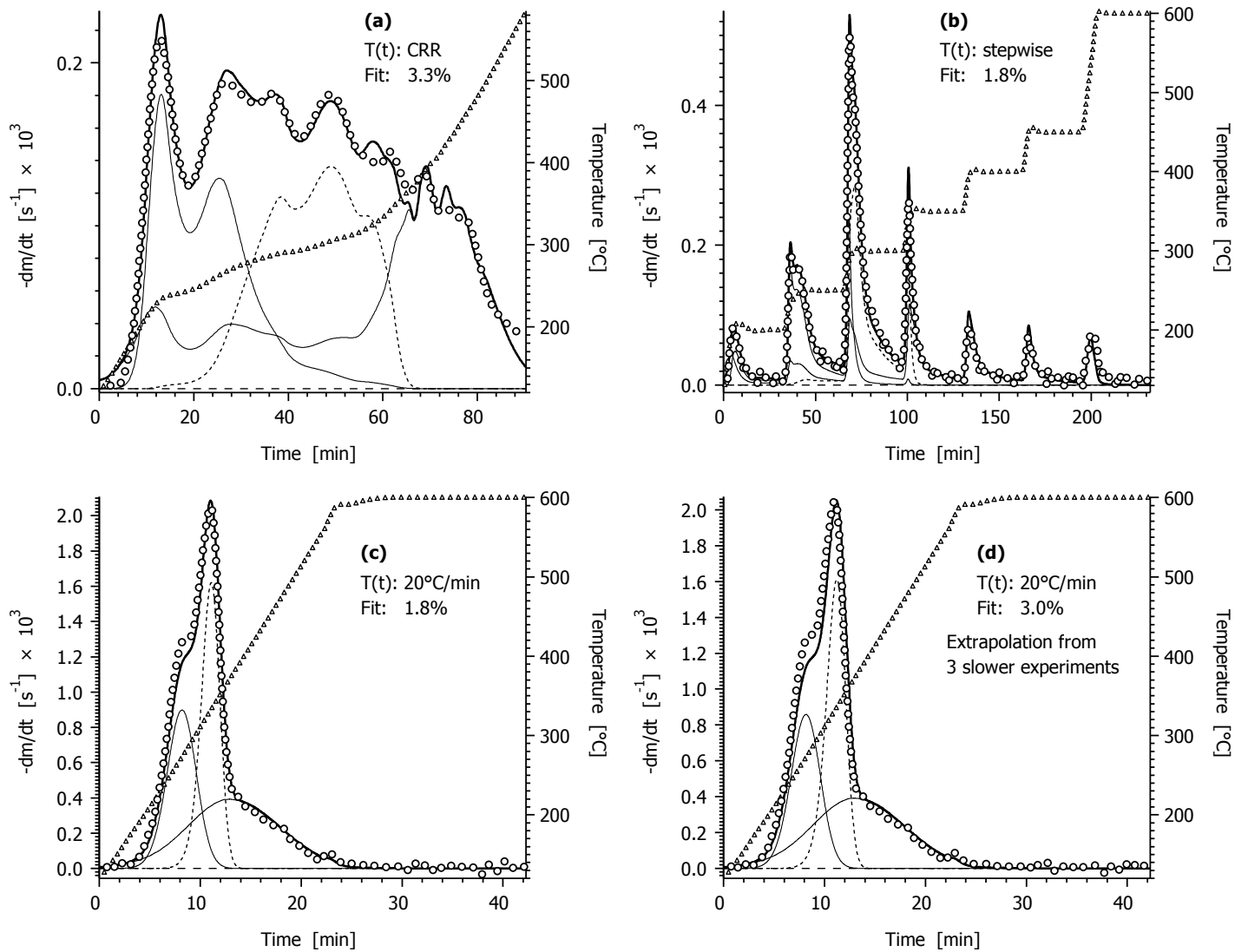


**Figure 5.** Description of the devolatilization of the coffee waste sample by three DAEM reactions. (See Figure 2 for notes and line styles.)

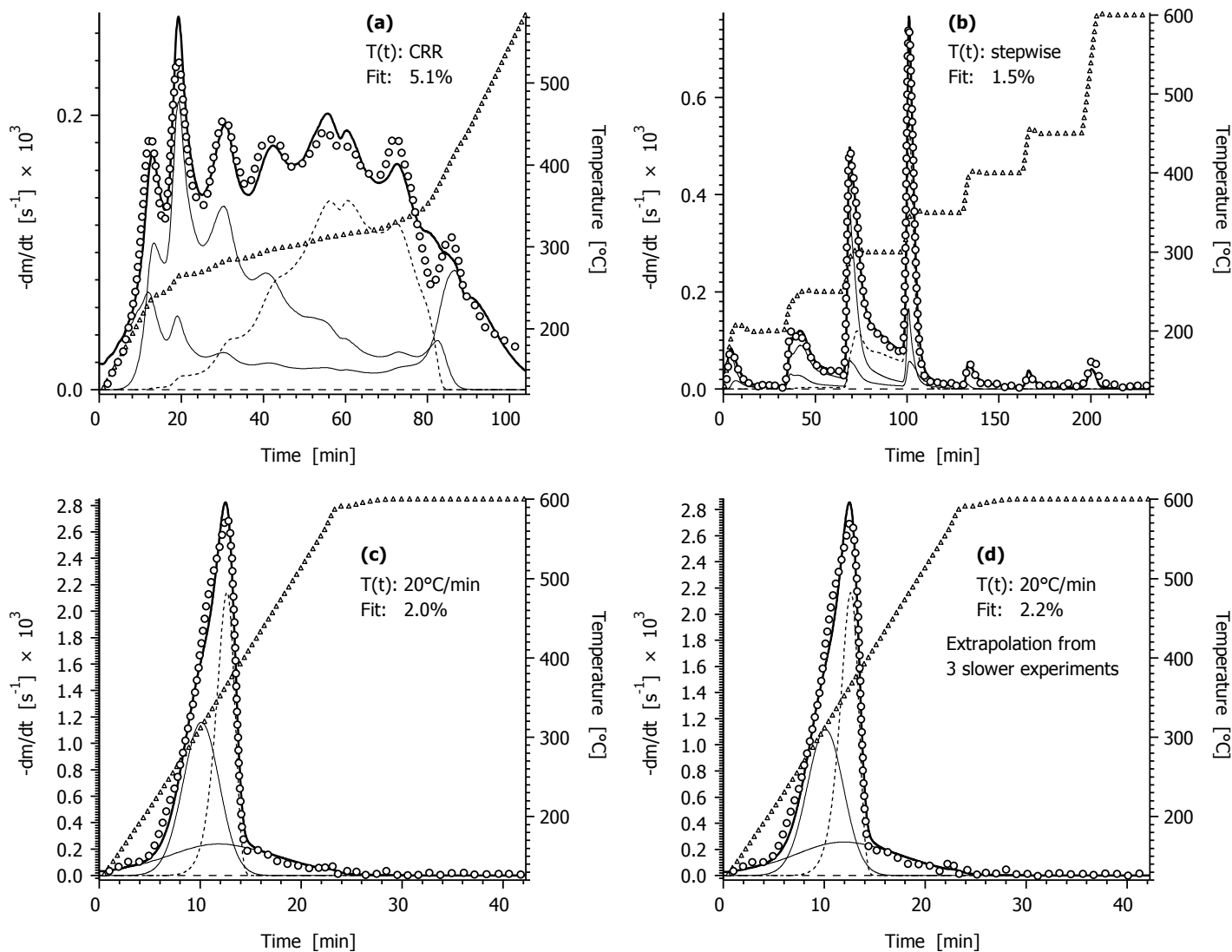


**Figure 6.** Description of the devolatilization of the fiberboard sample by three DAEM reactions. (See Figure 2 for notes and line styles.)

**3.6. Comparison of the models.** The good fit of the experimental data required the assumption of 7 – 8 pseudocomponents in the first order model. Accordingly, the fit of the experiments was achieved by the proper adjustment of 21 – 24 parameters ( $E_j$ ,  $A_j$  and  $c_j$  values were determined for each partial reaction). The application of the  $n$ th order kinetics for the partial reaction led to 4 partial peaks with 16 unknown parameters while only 3 pseudocomponents and 12 unknown parameters were required when the distributed activation energy model was employed for the partial reactions. In this respect the distributed activation energy model is the best of the models employed in the paper. The performance of this model was illustrated for all the samples. (See Figures 4 – 6.)

The extrapolation tests on the reliability of the models gave equally good results for all the three models employed, as it is shown in Table 6. The 1<sup>st</sup> column of data ( $\delta fit_{20^\circ C/min}$ ) expresses the efficiency of the extrapolation tests. (See the table footnotes for the details.) The rest of the data in Table 6 shows that the evaluation of the three slowest experiments results in roughly the same parameters as that of the whole set of experiments. Note that alterations of 7 – 11 kJ/mol cannot be regarded large in non-isothermal reaction

kinetics.<sup>51</sup> The results shown in Table 6 prove that the information content of the experiments is suitable for the reliable determination of the unknown parameters.

**Table 6. Comparison of the evaluations of three and five experiments<sup>a</sup>**

Model	$(\delta fit_{20^\circ C/min})_{rms}^b$ (%)	$(\delta c)_{rms}^c$	$(\delta E)_{rms}^{c,d}$ (kJ/mol)	$(\delta \log_{10} A)_{rms}^c$ ( $\log_{10} s^{-1}$ )	$(\delta n)_{rms}^c$	$(\delta \sigma)_{rms}^c$ (kJ/mol)
1 <sup>st</sup> order	0.8	0.01	11	0.9	–	–
power law	0.5	0.02	7	0.7	0.7	–
DAEM <sup>d</sup>	0.8	0.01	9	0.8	–	1.4

<sup>a</sup> All the three samples are included in the root mean square values of this table.

<sup>b</sup> The difference between the best fit and the fit in the extrapolation test was calculated for each 20°C/min experiment. The root mean square values of these differences are presented.

<sup>c</sup> The parameters obtained from the simultaneous evaluation of five and three experiments, respectively, were compared. The corresponding differences were calculated for each parameter at each sample. The root mean squares of these differences are presented.

<sup>d</sup> In the last row  $\delta E$  represents differences between the means of the activation energy distribution,  $E_{0,j}$ .

Finally the magnitude of the obtained activation energies is surveyed briefly. For this purpose we compare the averages of the obtained  $E_j$  values for each sample and each model in Table 7. It is interesting to note that the brewery and the coffee waste samples have very close average  $E$  values in each model, while the fiberboard has lower values. When the models are compared in this respect, one can note that the first order and the  $n$ th order kinetics resulted in similar magnitudes while DAEM results in much higher mean activation energies. Note that three models describe equally well the experiments in a wide range of  $T(t)$  temperature programs.

**Table 7. Comparison of the average activation energies<sup>a</sup>**

Sample	BSG	CW	MD F
1 <sup>st</sup> order	154	153	145
power law	164	165	136
DAEM	218	227	188

<sup>a</sup> Average activation energies (kJ/mol) were calculated for each model and each sample. In the last row the averages were formed from the means of the activation energy distribution,  $E_{0,j}$ .

**3.7. Do we need complicated models?** As outlined in Sections 3.5, the distributed activation energy models evidenced good performance with the assumption of only three partial processes. The distributions in this model describe approximately the distributed nature of various reacting species in the biomass wastes. (See the considerations at the beginning of Section 3.4, too.) The mathematical handling and numerical solution of a DAEM, however, is much more difficult than those of a first order model. The question arises: can we describe the data by three first order reactions, too, if we do not require a good fit between the experiments and the simulated curves? We carried out evaluations to clarify this question. It turned out that three first order reactions can give reasonable fit values (3.3-4.4%) if the evaluation is restricted only to the

linear  $T(t)$  experiments. (Note that most of the biomass kinetic studies in the literature have employed only linear heating.) However, this simple model gives rather poor results if we also require the description of sections with isothermal and irregularly changing temperatures. When the CRR, stepwise and linear  $T(t)$  experiments were evaluated simultaneously, the rms fit values for the whole series (as calculated from equations 1 – 2) were between 6.6 and 8.3. Besides, the extrapolation tests gave bad results. Figure 7 shows the fit of the 20°C/min BSG experiment by parameters obtained from all the five experiments (a) and by parameters obtained from the three slowest experiments (b).

Keeping in mind the recent huge development of the capabilities of computers and computing methods, we are convinced that the use of the complex kinetic models (like the  $n$ th order model with four reactions or a DAEM with 3 reactions) is a more promising way for modeling in R&D and industrial applications.

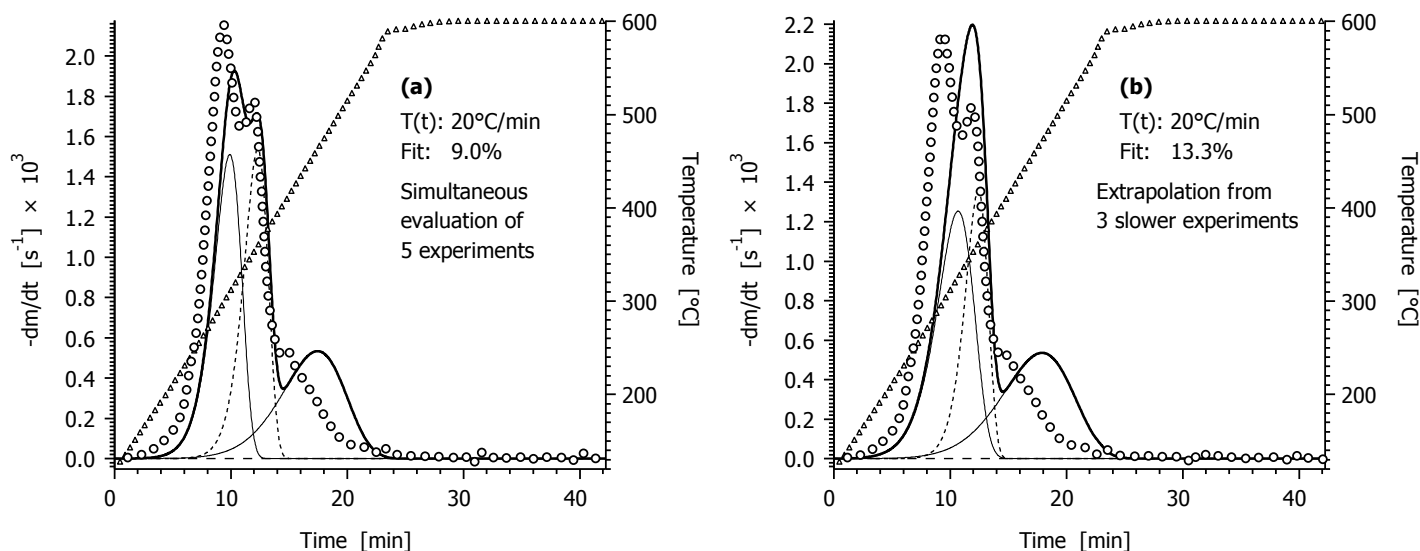


**Figure 7.** Approximate description of the devolatilization of the BSG sample by three first order reactions. (See Figure 2 for notes and line-styles).

## 4. Conclusions

(1) Three types of wastes were studied at five different  $T(t)$  temperature programs. The temperature programs covered a wide range of experimental conditions: the experiments exhibited 10 – 14 times variation in time span, mean reaction rate and peak reaction rate. The experiments on a given sample were described by the same set of model parameters. The optimal parameters were determined by the method of least squares. Three models were proposed that described equally well the behavior of the samples in the whole range of observations.

(2) A model built from three distributed activation energy reactions was suitable to describe the devolatilization at the highly different  $T(t)$  functions of our study with only 12 adjustable parameters. The other two models contained simpler mathematical equations (first order and  $n$ th order partial reactions, respectively), accordingly their use may be more convenient when the coupling of kinetic and transport equations are needed. On the other hand, the simpler models needed higher numbers of parameters to describe the complexity of these wastes

(3) The reliability of the proposed models was tested in three ways:

- (i) the models provided good fits for all the five experiments of a sample;
- (ii) the evaluation of a narrower subset of the experiments (the three slowest experiments) provided approximately the same parameters as the evaluation of the whole series of experiments;
- (iii) the models proved to be suitable to predict the behavior of the samples outside of those experimental conditions at which the model parameters were determined.

As outlined earlier, check (iii) corresponded to an extrapolation to ca. four-time higher reaction rates from the domain of the three slowest experiments.

(4) The evaluated experiments included “constant reaction rate” (CRR) measurements. This type of temperature control involves a continuously changing heating rate. The simultaneous evaluation of linear, stepwise and CRR experiments proved to be advantageous in the determination of reliable kinetic models.

(5) As outlined in the Introduction, the samples had very different chemical compositions. Nevertheless, the same models described them equally well. Accordingly, the models and the strategies for their evaluation and validation can be recommended for a wider range of biomass studies.

**Acknowledgment.** This work has been part of the “Environment and Process Management” research program, funded by the Research Council of Norway. The first author is grateful to the Nordic Graduate School of Biofuels Science and Technology (biofuelsGS) for providing financial support. The 2<sup>nd</sup> author acknowledges the support of the Hungarian National Research Fund (OTKA T37705).

## NOMENCLATURE

$\alpha_j$	reacted fraction of a pseudocomponent
$A_j$	pre-exponential factor ( $s^{-1}$ )
$c_j$	normalized mass of volatiles formed from a pseudocomponent
$E_j$	activation energy (kJ/mol)
$E_{0,j}$	mean activation energy in a distributed activation energy model (kJ/mol)
$fit$	$100 S^{0.5}$ (%)
$h_k$	height of a $-dm^{obs}/dt$ curve
$m$	normalized sample mass (dimensionless)
$m^{calc}(t)$	normalized sample mass calculated from a model
$m^{obs}(t)$	mass of the sample divided by the initial sample mass
$N_{comp}$	number of pseudocomponents
$N_{exp}$	number of experiments evaluated simultaneously
$N_k$	number of evaluated data on the $k$ th experimental curve
$R$	gas constant ( $8.3143 \times 10^{-3}$ kJ mol $^{-1}$ K $^{-1}$ )
$\sigma_j$	width parameter (variance) of Gaussian distribution
$S$	least squares sum
$t$	time (s)
$T$	temperature ( $^{\circ}C$ , K)

### Subscripts:

$i$	digitized point on an experimental curve
$j$	pseudocomponent
$k$	experiment
rms	root means square

## REFERENCES

- (1) González, J.F.; Encinar, J.M.; Canito, J.L.; Sabio, E.; Chacón, M. Pyrolysis of cherry stones: energy uses of the different fractions and kinetic study. *J. Anal. Appl. Pyrolysis* **2003**, *67*, 165-190.
- (2) Saenger, M.; Hartge, E.-U.; Werther, J.; Ogada, T.; Siagi, Z. Combustion of coffee husks. *Renewable Energy* **2001**, *23*, 103-121.
- (3) Fang, M.; Yang, L.; Chen, G.; Shi, Z.; Luo, Z.; Cen, K. Experimental study on rice husk combustion in a circulating fluidized bed. *Fuel Process. Technol.* **2004**, *85*, 1273-1282.
- (4) Özbay, N.; Pütün, A.E.; Uzun, B.B.; Pütün, E. Biocrude from biomass: pyrolysis of cottonseed cake. *Renewable Energy* **2001**, *24*, 615-625.
- (5) Silva, M.A.; Nebra, S.A.; Machado Silva, M.J.; Sanchez, C.G. The use of biomass residues in the Brazilian soluble coffee industry. *Biomass Bioenergy* **1998**, *14*, 457-467.
- (6) Di Blasi, C.; Signorelli, G.; Di Russo, C.; Rea G. Product distribution from pyrolysis of wood and agricultural residues. *Ind. Eng. Chem. Res.* **1999**, *38*, 2216-2224.

- (7) Bridgwater, A.V. Renewable fuels and chemicals by thermal processing of biomass. *Chem. Eng. J.* **2003**, *91*, 87-102.
- (8) Várhegyi, G; Antal Jr, M.J.; Székely, T.; Szabó, P. Kinetics of the thermal decomposition of cellulose, hemicellulose, and sugarcane bagasse. *Energy Fuels* **1989**, *3*, 329-335.
- (9) Balci, S; Dogu, T.; Yucal, H. Pyrolysis kinetics of lignocellulosic materials. *Ind. Eng. Chem. Res.* **1993**, *32*, 2573-2579.
- (10) Garcia, A.N.; Marcilla, A.; Font, R. Thermogravimetric kinetic study of the pyrolysis of municipal solid waste. *Thermochim. Acta* **1995**, *254*, 277-304.
- (11) Cozzani, V.; Petarca, L.; Tognotti, L. Devolatilization and pyrolysis of refuse derived fuels: characterization and kinetic modelling by a thermogravimetric and calorimetric approach. *Fuel* **1995**, *74*, 903-912.
- (12) Reynolds, JG; Burnham, AK; Wallman, PH. Reactivity of paper residues produced by a hydrothermal pretreatment process for municipal solid wastes. *Energy Fuels* **1997**, *11*, 98-106
- (13) Várhegyi, G; Antal Jr, M.J.; Jakab, E.; Szabó, P. Kinetic modeling of biomass pyrolysis. *J. Anal. Appl. Pyrolysis* **1997**, *42*, 73-87.
- (14) Lin, K.-S.; Wang, H. P.; Liu, S.-H.; Chang, N.-B.; Huang, Y.-J.; Wang, H.-C. Pyrolysis kinetics of refuse-derived fuel. *Fuel Process. Technol.* **1999**, *60*, 103-110.
- (15) Helsen, L.; Van den Bulck, E. Kinetics of the low-temperature pyrolysis of chromated copper arsenate-treated wood. *J. Anal. Appl. Pyrolysis* **2000**, *53*, 51-79.
- (16) Sørum, L.; Grønli, M.G.; Hustad, J.E. Pyrolysis characteristics and kinetics of municipal solid wastes. *Fuel* **2001**, *80*, 1217-1227.
- (17) Stenseng, M; Jensen, A.; Dam-Johansen, K. Investigation of biomass pyrolysis by thermogravimetric analysis and differential scanning calorimetry. *J. Anal. Appl. Pyrolysis* **2001**, *58-59*, 765-780.
- (18) Manyà, J. J.; Velo, E.; Puigjaner, L. Kinetics of biomass pyrolysis: A reformulated three-parallel-reactions model. *Ind. Eng. Chem. Res.* **2003**, *42*, 434-441.
- (19) Jauhiainen, J.; Conesa, J.A.; Font, R.; Martin-Gullon, I. Kinetics of the pyrolysis and combustion of olive oil solid waste. *J. Anal. Appl. Pyrolysis* **2004**, *72*, 9-15.
- (20) Gómez, C. J.; Várhegyi, G.; Puigjaner, L. Slow pyrolysis of woody residues and an herbaceous biomass crop: A kinetic study. *Ind. Eng. Chem. Res.* **2005**, *44*, 6650-6660.
- (21) Skodras, G.; Grammelis, O. P.; Basinas, P.; Kakaras, E.; Sakellariopoulos, G. Pyrolysis and combustion characteristics of biomass and waste-derived feedstock. *Ind. Eng. Chem. Res.* **2006**, *45*, 3791-3799.
- (22) Yang, H; Yan, R.; Chen, H.; Zheng, C.; Lee D.H.; Liang, D.T. In-depth investigation of biomass pyrolysis based on three major components: hemicellulose, cellulose and lignin. *Energy Fuels* **2006**, *20*, 388-393.
- (23) Burnham, A. K.; Braun, R. L. Global kinetic analysis of complex materials. *Energy Fuels* **1999**, *13*, 1-22.
- (24) Caballero, J. A.; Conesa, J. A. Mathematical considerations for non-isothermal kinetics in thermal decomposition. *J. Anal. Appl. Pyrolysis* **2005**, *73*, 85-100.
- (25) Várhegyi, G. Aims and methods in non-isothermal reaction kinetics. *J. Anal. Appl. Pyrolysis* **2007**. Available in the online edition of the journal as article in press: doi:10.1016/j.jaap.2007.01.007
- (26) Grøndal, J. Utilization of brewers spent grains fractions as ingredients in the food and feed industry. An industrial research education programme under the Danish academy of technical sciences, project No. 244, **1990**.
- (27) European Union's Survey on Agricultural Markets, 2005. Published in the homepage of the European Commission: [http://ec.europa.eu/agriculture/markets/hops/index\\_en.htm](http://ec.europa.eu/agriculture/markets/hops/index_en.htm).
- (28) Fuller, B. Global panel markets: China's growing role as consumer and supplier. 38th International Wood Composites Symposium, **2004**. (Available on the internet: <http://www.woodsymposium.wsu.edu/conference/2004Archive.html>.)
- (29) Mussatto, S. I.; Dragone, G.; Roberto, I.C. Brewers' spent grain: generation, characteristics and potential applications. *J. Cereal Sci.* **2006**, *43*, 1-14.
- (30) Mbagwu, J.S.C.; Ekwealor, G.C. Agronomical potential of brewers' spent grains. *Biol. Wastes* **1990**, *34*, 335-347.

- (31) Hirata, T; Kawamoto, S.; Okuro, A. Pyrolysis of melamine-formaldehyde and urea-formaldehyde resins. *J. Appl. Polym. Sci.* **1991**, *42*, 3147-3163.
- (32) Werther, J.; Saenger, M.; Hartge, E.-U.; Ogada, T.; Siagi, Z. Combustion of agricultural residues. *Prog. Energ. Comb. Sci.* **2000**, *26*, 1-27.
- (33) Gan, Q.; Allen, S. J.; Matthews, R. Activation of waste MDF sawdust charcoal and its reactive dye adsorption characteristics. *Waste Manag.* **2004**, *24*, 841-848.
- (34) Becidan, M.; Skreiberg, Ø.; Hustad, J.E. Products distribution and gas release in pyrolysis of thermally thick biomass residues samples. *J. Anal. Appl. Pyrolysis* **2007**, *78*, 207-213.
- (35) Santos, M.; Jiménez, J. J.; Bartolomé, B.; Gómez-Cordovés, C.; del Nozal, M.J. Variability of brewer's spent grain within a brewery. *Food Chemistry* **2003**; *80*, 17-21.
- (36) Illy, A.; Viani, R. Espresso Coffee. The chemistry of quality. Academic press Third printing 1998.
- (37) Broido, A.; Nelson, M. A. char yield on pyrolysis of cellulose *Comb. Flame* **1975**, *24*, 263-268.
- (38) Burnham, A. K.; Weese, R. K. Kinetics of thermal degradation of explosive binders Viton A, Estane, and Kel-F. *Thermochim. Acta* **2005**, *426*, 85-92.
- (39) Mészáros. E.; Várhegyi, G; Jakab, E; Marosvölgyi, B. Thermogravimetric and reaction kinetic analysis of biomass samples from an energy plantation. *Energy Fuels* **2004**, *18*, 497-507.
- (40) Várhegyi, G.; Till, F. Computer processing of thermogravimetric - mass spectrometric and high pressure thermogravimetric data. Part 1. Smoothing and differentiation. *Thermochim. Acta* **1999**, *329*, 141-145.
- (41) Várhegyi, G.: Kinetic evaluation of non-isothermal thermoanalytical curves in the case of independent reactions. *Thermochim. Acta* **1979**, *28*, 367-376.
- (42) Várhegyi, G.; Szabó, P.; Antal, M. J., Jr.: Kinetics of charcoal devolatilization. *Energy Fuels* **2002**, *16*, 724-731.
- (43) Várhegyi, G.; Szabó, P.; Antal, M. J., Jr. Reaction kinetics of the thermal decomposition of cellulose and hemicellulose in biomass materials. In *Advances in Thermochemical Biomass Conversion* (Ed. by A. V. Bridgwater), Volume 2, Chapman and Hall: London, **1994**, pp. 760-771.
- (44) Caballero, J. A.; Font, R.; Marcilla, A. Comparative study of the pyrolysis of almond shells and their fractions, holocellulose and lignin. Product yields and kinetics. *Thermochim. Acta* **1996**, *276*, 57-77.
- (45) Caballero, J. A.; Conesa, J. A.; Font, R.; Marcilla, A. Pyrolysis kinetics of almond shells and olive stones considering their organic fractions. *J. Anal. Appl. Pyrol.* **1997**, *42*, 159-175.
- (46) Teng, H.; Lin, H. C., Ho, J. A. Thermogravimetric analysis on global mass loss kinetics of rice hull pyrolysis. *Ind. Eng. Chem. Res.* **1997**, *36*, 3974-3977.
- (47) Órfão, J. J. M.; Antunes, F. J. A.; Figueiredo, J. L. Pyrolysis kinetics of lignocellulosic materials – Three independent reactions model. *Fuel* **1999**, *78*, 349-358.
- (48) Vamvuka, D.; Pasadakis, N.; Kastanaki E. Kinetic modeling of coal/agricultural by-product blends. *Energy Fuels* **2003**, *17*, 549 -558.
- (49) IUPAC Compendium of Chemical Terminology, 2<sup>nd</sup> Edition, International Union of Pure and Applied Chemistry, 1997. Available on the internet: <http://www.iupac.org/publications/compendium/index.html>.
- (50) Müller-Hagedorn, M; Bockhorn, H.; Krebs, L.; Müller. U. A comparative kinetic study on the pyrolysis of three different wood species. *J. Anal. Appl. Pyrolysis* **2003**, *68-69*, 231-249.
- (51) Grønli, M.; Antal, M. J., Jr.; Várhegyi, G.: A round-robin study of cellulose pyrolysis kinetics by thermogravimetry. *Ind. Eng. Chem. Res.* **1999**, *38*, 2238-2244.